THE JOURNAL OF BIOLOGICAL CHEMISTRY VOL. 286, NO. 33, pp. 28978–28987, August 19, 2011

A Red-shifted Antenna Protein Associated with Photosystem II in *Physcomitrella patens*[*] [S]

Received for publication, February 4, 2011, and in revised form, June 23, 2011 Published, JBC Papers in Press, June 24, 2011, DOI 10.1074/jbc.M111.226126

Alessandro Alboresi[‡], Caterina Gerotto[§], Stefano Cazzaniga[‡], Roberto Bassi[‡¶1], and Tomas Morosinotto[§]

From the [‡]Dipartimento di Biotecnologie, Università di Verona, Strada le Grazie 15, 37134 Verona, Italy, the [§]Dipartimento di Biologia, Università di Padova, Via Ugo Bassi 58 B, 35121 Padova, Italy, and [¶]ICG-3, Phytosphäre Forschungszentrum Jülich, 52425 Jülich, Germany

Antenna systems of plants and green algae are made up of pigment-protein complexes belonging to the light-harvesting complex (LHC) multigene family. LHCs increase the light-harvesting cross-section of photosystems I and II and catalyze photoprotective reactions that prevent light-induced damage in an oxygenic environment. The genome of the moss *Physcomitrella patens* contains two genes encoding LHCb9, a new antenna protein that bears an overall sequence similarity to photosystem II antenna proteins but carries a specific motif typical of photosystem I antenna proteins. This consists of the presence of an asparagine residue as a ligand for Chl 603 (A5) chromophore rather than a histidine, the common ligand in all other LHCbs. Asparagine as a Chl 603 (A5) ligand generates red-shifted spectral forms associated with photosystem I rather than with photosystem II, suggesting that in *P. patens*, the energy landscape of photosystem II might be different with respect to that of most green algae and plants. In this work, we show that the *in vitro* refolded LHCb9-pigment complexes carry a red-shifted fluorescence emission peak, different from all other known photosystem II antenna proteins. By using a specific antibody, we localized LHCb9 within PSII supercomplexes in the thylakoid membranes. This is the first report of red-shifted spectral forms in a PSII antenna system, suggesting that this biophysical feature might have a special role either in optimization of light use efficiency or in photoprotection in the specific environmental conditions experienced by this moss.

Light energy powers photosynthesis. Sunlight is absorbed by chlorophyll (Chl)[2] and carotenoid molecules bound to protein supercomplexes embedded in thylakoid membranes, called photosystem I and II (PSI and PSII). Each photosystem has two moieties: (i) the core complex and (ii) the peripheral antenna system. The core complex contains mostly plastid-encoded subunits, which are responsible for charge separation and for the first steps of electron transport and are also active in light harvesting. An additional antenna system, made of nucleus-encoded subunits binding Chl *a*, Chl *b*, and xanthophylls, is localized peripherally in photosystems and is responsible for most light harvesting, transfer of excitation energy to the reaction centers, and photoprotective reactions like ROS scavenging and quenching of triplet and singlet excited states (1–3). Reaction center protein sequences are widely conserved among organisms, and only small differences are found in sequences of oxygenic organism as far apart as higher plants and cyanobacteria (4, 5). Antenna systems are instead more variable, and in land plants and green algae, they are composed of multiple copies of light-harvesting complex (LHC) proteins (4) assembled around core complexes (6). Clustering analysis of LHC protein sequences clearly distinguishes members associated with PSI (LHCa or LHCI) from those belonging to PSII (LHCb or LHCII) (7). In *Arabidopsis thaliana*, six different polypeptides were identified for PSI (LHCa1 to -6) and a total of eight for PSII (LHCb1 to -8), including the more recent proposed addition of LHCb7 and LHCb8 (7, 8). In the genome of the moss *Physcomitrella patens*, two sequences encoding an additional LHCb protein, named LHCb9, were also identified (9).

The fluorescence emission spectrum of plant thylakoids at low temperature shows two main emission peaks (*i.e.* 685 and 735 nm), which originate from the grana domains containing PSII-LHCII complexes and the stroma-exposed domains containing PSI-LHCI, respectively. The PSI emission originates from Chl *a* molecules absorbing at wavelengths higher than 700 nm, thus strongly red-shifted with respect to Chl *a* molecules in organic solvents. For this reason, they are often called "red Chls" or "red (spectral) forms." Red Chls have been localized in the PSI antenna system, particularly in LHCa3 and LHCa4 (10–13). Mutational analysis showed that red forms in LHCa complexes originate from two interacting Chls, 603 and 609 (also known as A5 and B5 in a previous nomenclature)[3] (17, 18). The nature of the ligand of Chl 603 plays a key role in the origin of "red" forms by determining the distance between the α-carbon chain and the bound chlorophyll. In fact, an asparagine coordinates Chl 603 in LHCa3 and LHCa4 and it holds the chro-

* This work was supported by the Cassa di Risparmio di Padova e Rovigo (CaRiPaRo) Foundation, Università di Padova Grant CPDA089403, EEC Project Harvest and Fondo per gli Investimenti della Ricerca di Base-Parallelomics Grant RBIP06CTBR.

[S] The on-line version of this article (available at http://www.jbc.org) contains supplemental Fig. 1.

[1] To whom correspondence should be addressed: Dipartimento di Biotecnologie, Università di Verona, Strada le Grazie 15, 37134 Verona, Italy. Tel.: 39-0458027915; Fax: 39-0458027929; E-mail: roberto.bassi@univr.it.

[2] The abbreviations used are: Chl, chlorophyll; LHC, light-harvesting complex; Lhca and -b, light-harvesting complex of photosystem I and II, respectively; LHCII, major light harvesting complex of photosystem II; PSI and PSII, photosystem I and II, respectively; Tricin, *N*-[Tris-(hydroxymethyl)-methyl]glycine; LT, low temperature.

[3] Different nomenclatures have been proposed for Chl binding sites in LHC proteins. Here we use the one from Ref. 14 instead of the older one from Ref. 15 because the latter suggests occupancy of the site by Chl *a* or *b* which is not a general property through the protein family. We also do not use the one from Ref. 16 because it refers specifically to plant PSI antennas and could not be generalized to other homologous proteins.

mophore in a position allowing its strong interaction with Chl 609, which leads to formation of a charge transfer state and the appearance of red emission forms (18–20). In LHCa1 and LHCa2, the coordination by the bulkier histidine puts Chls 603 away from Chl 609, leading to a weaker interaction and a strong reduction of red forms (18). LHCb1 to -8 polypeptides, composing the antenna system of photosystem II, all have a histidine as Chl 603 ligand and do not show red-shifted emissions. LHCb9 is an exception because it carries an asparagine residue as the ligand for this chlorophyll (9). In this work, we report on the characterization of the two LHCb9 isoforms encoded in the *P. patens* genome. The cDNA sequence was overexpressed in bacteria and reconstituted *in vitro* with pigments. The holoprotein showed a fluorescence emission peak red-shifted with respect to any other LHCb protein thus far described. We also show that LHCb9 is found in *P. patens* thylakoids and is indeed associated with PSII, in agreement with its overall sequence similarity to LHCb proteins. The possible function of red-shifted spectral forms in PSII and the reason for their presence in *P. patens* is discussed with reference to the adaptation of antenna systems to environmental growth conditions.

EXPERIMENTAL PROCEDURES

Sequence Retrieval and Analysis—LHCb9 and other LHC sequences from *P. patens* were retrieved from expressed sequence tag (PHYSCObase) and genome (Department of Energy Joint Genome Institute) databases as described (9, 21). Sequence information from the National Center for Biotechnology Information and The Plant Transcript Assemblies were mainly used for TBLASTN searches. Sequence alignments were generated by ClustalW and manually corrected using BioEdit. The regions of the three transmembrane helices were considered in the analysis, as described previously in similar works (22, 23). Phylogenetic trees were inferred using parsimony, neighbor-joining distance, and maximum likelihood approaches using the Phylogenetic Inference Package (PHYLIP) version 3.67 and the PHYML program (24, 25), as described previously (9).

Reconstitution in Vitro—LHCb9.1 (XM_001756491) and LHCb9.2 (XM_001779101) were amplified by PCR from total *P. patens* cDNA and cloned in a modified pET-28a(+) (26). The apoprotein was overexpressed in *E. coli* and purified as inclusion bodies. Pigment-protein complexes were refolded *in vitro* and purified from excess free pigments (27). The N164H mutant for LHCb9.2 (numbers refer to the precursor sequence) was obtained using the QuikChange™ site-directed mutagenesis kit (Stratagene).

Spectroscopy and Pigment Analysis—Absorption spectra were recorded using a Cary 300 (Varian Inc.) spectrophotometer, in 10 mM HEPES, pH 7.5, 0.2 M sucrose, and 0.06% *n*-dodecyl-β-D-maltopyranoside. Low temperature fluorescence emission spectra were measured using a Cary Eclipse (Varian Inc.) and corrected for the instrumental response. Samples were excited at 440, 475, and 500 nm. The spectral bandwidth was 5 nm (excitation) and 3 nm (emission). Chlorophyll concentration was about 0.02 μg/ml in 60% glycerol, 10 mM HEPES, and 0.03% *n*-dodecyl-β-D-maltopyranoside. Chlorophyll/carotenoid ratio and Chl *a*/*b* ratio were independently measured by fitting the spectrum of acetone extracts with the spectra of individual purified pigments (28) and by HPLC analysis (29).

Physcomitrella Growth and Thylakoid Isolation—Protonemal tissue of *P. patens*, Gransden wild-type strain, was grown on PpNO3 minimum medium (30) solidified by 1% purified agar agar (Euromedex, Mundolsheim, France). Plants were propagated under sterile conditions on minimum medium in 9-cm Petri dishes overlaid with a cellophane disk (Cannings, Bristol, UK) as described (31). Plates containing plant samples were placed in a growth chamber under controlled conditions: 22 °C day/21 °C night temperature, 16 h light/8 h dark photoperiod, and a light intensity of 40 microeinsteins m^{-2} s^{-1} (10 microeinsteins m^{-2} s^{-1} for low light and 400 microeinsteins m^{-2} s^{-1} for high light). Thylakoids from 2-week-old plants (protonemal tissue) were prepared following the same protocol used for higher plants with minor modifications. Tissues were harvested and freshly homogenized in cold extraction buffer (0.5% milk powder, 0.4 M NaCl, 20 mM Tricine-KOH, pH 7.8, and 1 mM ϵ-aminocaproic acid). After filtration, samples were precipitated by centrifugation at 4 °C at 1500 × *g* for 15 min and then resuspended in an ipotonic buffer (15 mM NaCl, 5 mM $MgCl_2$, and 20 mM Tricine-KOH, pH 7.8). After centrifugation for 15 min at 4 °C at 10,000 × *g*, thylakoids were resuspended in a buffer containing 50% glycerol, 15 mM NaCl, 5 mM $MgCl_2$, and 10 mM Hepes-KOH, pH 7.5. Thylakoids were frozen in liquid nitrogen and stored at −80 °C until use. Purification of pigment-binding proteins from thylakoids was performed by sucrose gradient ultracentrifugation upon solubilization of membranes with final 0.8% *n*-dodecyl-α-D-maltopyranoside.

SDS-PAGE Electrophoresis, Western Blotting Analysis, and Stoichiometry Calculations—SDS-PAGE analyses were performed as in Ref. 32. After SDS-PAGE, polypeptides were transferred onto a nitrocellulose membrane (Sartorious AG, Gottingen, Germany) using a blot system from Bio-Rad and detected with specific homemade antibodies (supplemental Fig. 1). To verify the identity of the LHCb9 band, antibody was preincubated for 1 h with total 35 μg of LHCb9.1 and LHCb9.2 inclusion bodies (17.5 μg each). In order to evaluate protein stoichiometry, we loaded 0.05, 0.03, 0.02, and 0.01 μg of Chl reconstituted protein together with 1.5, 1, 0.75, and 0.5 μg of Chl from thylakoids. Antibody signal was quantified by densitometry after checking its linearity with gel loading as in Ref. 33. In order to estimate LHCb9/PSII stoichiometry, we assumed that LHCb9 binds 10 ± 2 Chls/monomer. We also estimated *Physcomitrella* PSII antenna size using fluorescence induction in 3-(3,4-dichlorophenyl)-1,1-dimethylurea, whose kinetics are known to depend on the PSII functional antenna size. As a comparison, we used barley plants, WT and *clorina f2* mutants, where PSII antenna size is known to be 300 and 50 Chls/PSII, respectively (34). With this method, we could estimate PSII antenna size in *Physcomitrella* to be 529 ± 89 Chls/PSII. Final estimation is derived from green gels, like the ones in Ref. 9, showing that 68% of thylakoid Chls are associated with PSII core or antenna complexes. The latter two values led to the calculation that in *Physcomitrella* thylakoids, there are 788 ± 132 Chls present for each PSII.

Molecular Modeling—The LHCII structure from Ref. 14, Protein Data Bank accession code 1RWT, was mutated using

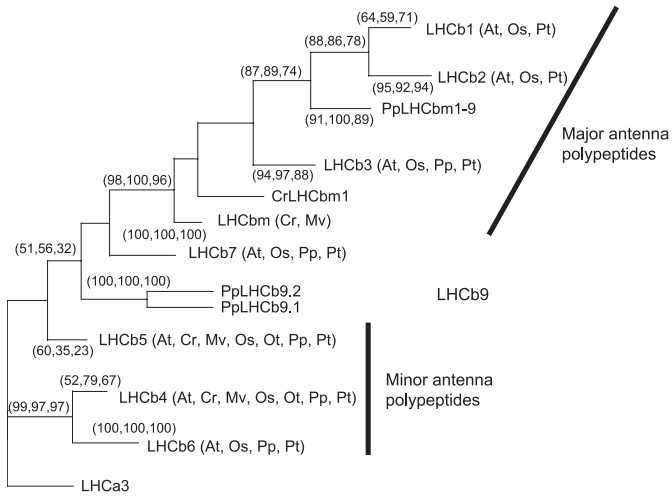

FIGURE 1. **Phylogenetic analysis of LHC polypeptides.** The evolutionary tree comparative analysis includes protein sequences from *A. thaliana* (*At*), *Populus trichocarpa* (*Pt*), *Oryza sativa* (*Os*), *P. patens* (*Pp*), *C. reinhardtii* (*Cr*), and *Ostreococcus tauri* (*Ot*). Sequences obtained from expressed sequence tag databases of a further algal species (*Mesostigma viride* (*Mv*)) were also included. LHCa3 from *A. thaliana*, *P. patens*, and *C. reinhardtii* was included as an external outgroup. The tree was built using a maximum likelihood approach. Bootstrap values reported in *brackets* were obtained from maximum likelihood, neighbor-joining distance, and maximum parsimony approaches, respectively. For clarity, these values are not shown when consistency is low or when nodes are not significant for isoform discrimination.

Swiss-PdbViewer (35). After mutating histidine into asparagine, the distance between Chl and protein backbone was manually corrected and fixed equal to Chl 612, which is also coordinated by asparagine.

RESULTS

A New LHC Polypeptide Identified in P. patens—LHCb9 was identified in the *P. patens* genome as carrying peculiar sequence properties with respect to any other previously known LHC isoform (9). The polypeptide sequence showed a similarity to PSII antenna polypeptides and was thus called LHCb9. We identified two isoforms, *LHCb9.1* and *LHCb9.2*, with 80% sequence identity. We observed that the number of expressed sequence tag clones identified in *P. patens* databases is particularly high for both *LHCb9* isoforms; *LHCb9.1* is the most abundant transcript among antenna proteins (9). Assuming that the number of expressed sequence tag clones retrieved is roughly indicative of gene expression levels (8), *LHCb9.1* is thus presumably a highly expressed *LHC* gene in *P. patens*, suggesting a relevant functional role for the corresponding polypeptide in the moss photosynthetic apparatus.

In Fig. 1, the sequence of LHCb9 is compared with those of other LHCb proteins. In the phylogenetic tree, LHCb9 sequences are located between monomeric LHCb proteins (LHCb4, LHCb5, and LHCb6) and the components of the major LHCII antenna complex (named LHCbm1 to -13 in *P. patens*). In fact, although LHCb9 sequences cluster with major antenna polypeptides, the consistency of this configuration is low, ranging from 32 to 56–100, depending on the algorithm employed. In fact, LHCb9.1 has 50% similarity and 30% identity with both sequences encoding major antenna polypeptides (*i.e.* PpLHCbm1 and -2 and PpLHCb3) and the minor antenna protein PpLHCb5. Similarity is instead lower when compared with PpLHCb4 and PpLHCb6 sequences.

Sequence analysis is useful to infer information on protein biochemistry and activity. We therefore looked closer at Chl-binding residues highly conserved in LHCs (14, 15, 36) and found that they are all conserved in LHCb9 (Fig. 2). An LHCb9 peculiarity is that Chl 603 is coordinated by an asparagine rather than a histidine as in all other LHCb polypeptides. Because both asparagine and histidine can coordinate the Mg^{2+} in Chl rings, pigment binding is probably unaffected (Fig. 2). A further characteristic of LHCb9 is the non-conservation of the histidine residue, as reported for LHCb6 polypeptide (7). It should be noticed, however, that an extra histidine is found in a nearby position in helix D and could coordinate Chl 614 according to the hypothesis that helix D assumes a different orientation than in other LHC proteins (Fig. 2).

Xanthophyll coordination in LHC proteins is most likely due to multiple interactions with the polypeptide, and sequence motifs for carotenoid binding are not well defined yet. Sites L1 and L2 are conserved in all LHC members analyzed so far (37, 38) and are likely to be present in LHCb9 as well. A conserved tyrosine residue in LHCb1, LHCb4, and LHCb5 has been shown to be fundamental for neoxanthin binding to site N1 (26). This tyrosine is also conserved in LHCb9 (position 209; Fig. 2), suggesting that it binds neoxanthin.

The capacity of LHCII polypeptides to form trimers depends on the presence of residues in the N-terminal domain WYR (indicated as a trimerization motif in Fig. 2) (39). A WYR motif is also found in LHCb5, although this is normally associated with PSII as a monomer (40) and only trimerizes in LHCII-depleted plants (41). In LHCb9, the first tryptophan of the motif is substituted by a tyrosine, suggesting a low probability of finding trimers, including LHCb9, in *P. patens* WT thylakoids.

In Vitro Reconstitution of LHCb9 Recombinant Protein—The presence of an asparagine replacing the more common histidine as a ligand for Chl 603 is typical of LHC members associated with PSI, such as *A. thaliana* LHCa3 and LHCa4 (9, 42), and LHCa2, LHCa4, and LHCa9 in *Chlamydomonas reinhardtii* (43). The asparagine in PSI antenna is responsible for red-shifted Chl absorption (18), and up to now, LHCb9 is the only case where this ligand for Chl 603 is found outside the LHCa subfamily.

In order to verify if the asparagine ligand can induce red-shifted Chl spectral forms even within a LHCb-like sequence, we cloned and expressed the two LHCb9 isoforms in *E. coli* using total *P. patens* cDNA as a template. LHCb9 apoproteins were purified from inclusion bodies and refolded *in vitro* in the presence of pigments using a well established procedure (27). Both LHCb9 polypeptides yielded stable monomeric pigment-binding proteins. Pigment compositions of the reconstituted complexes are reported in Table 1, together with reference data from *Hordeum vulgare* LHCb2 reconstituted *in vitro* using the same procedure (44). HvLHCb2 was chosen because its primary sequence is the most similar to LHCb9 among the LHCb isoforms characterized previously. Chl *a*/*b* ratios are very similar in all complexes (from 1.4 to 1.5; Table 1), suggesting that LHCb9 has a high affinity for Chl *b*, similar to LHCII members and different from monomeric LHCs, which have a higher Chl

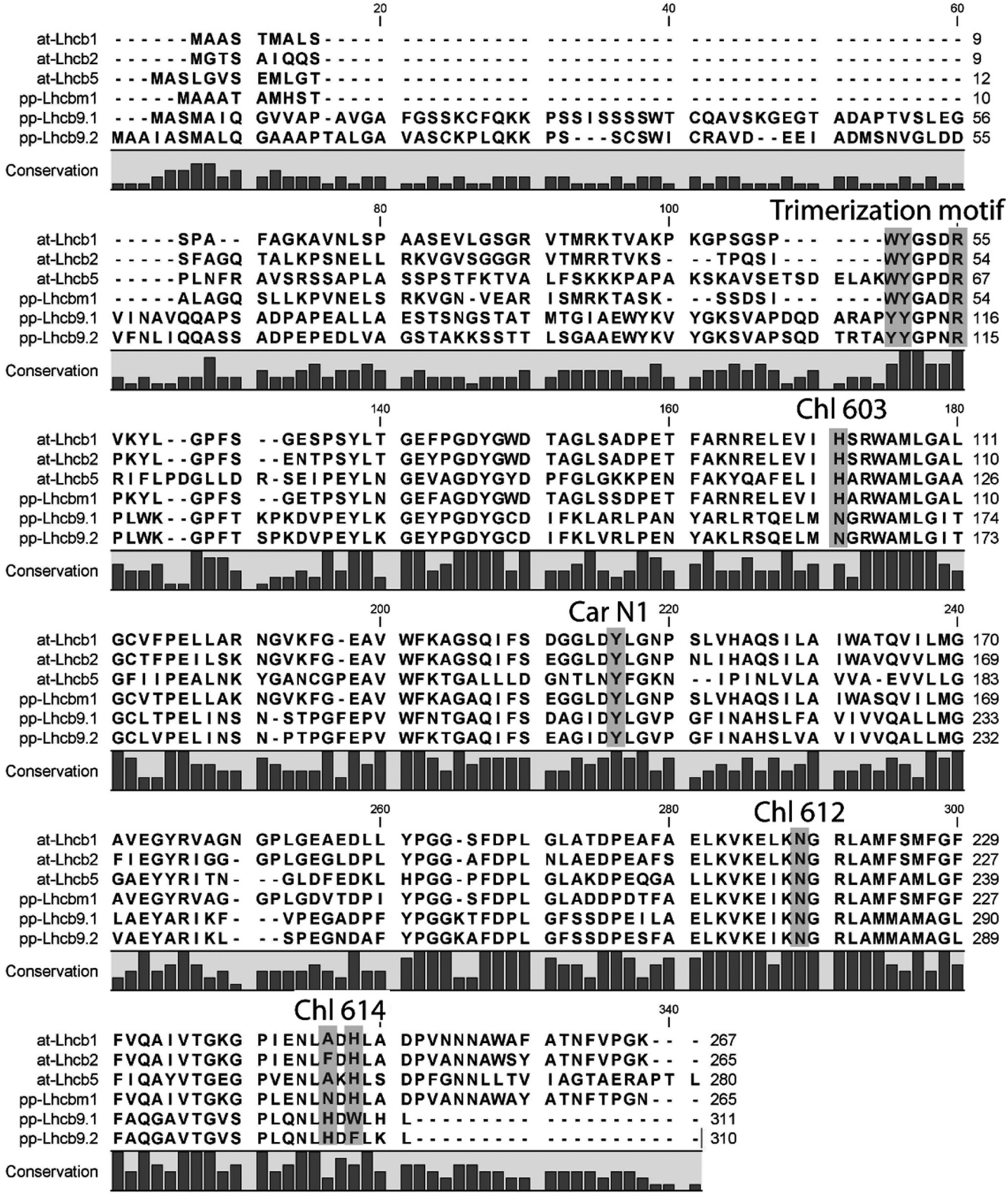

FIGURE 2. **Chlorophyll and carotenoid binding sites in LHCb9 sequence.** LHCb9.1 and LHCb9.2 polypeptide sequences have been aligned with LHCb1, LHCb2, and LHCb5 from *A. thaliana* and LHCbm1 from *P. patens*. The putative trimerization motif as well as residues known to be involved in coordination of Chl and carotenoid (*Car*) are indicated and discussed under "Results."

a/*b* ratio (*i.e.* a Chl *a*/*b* ratio of 2.0–2.2 and 3.0 for LHCb5 and LHCb4, respectively) (26, 45). In contrast, xanthophyll-binding properties of LHCb9 are more similar to those of minor LHCbs because it preferentially binds violaxanthin and lutein, whereas neoxanthin content is low with respect to LHCb2, a component of the major LHCII trimeric antenna.

Chl/protein binding stoichiometry of LHCb9 is not known, but it is most likely comprised between 9 and 12 Chls/mono-

TABLE 1

Pigment binding properties of LHCb9 reconstituted *in vitro*

Chl and carotenoid binding properties are reported for reconstituted LHCb9.1 and LHCb9.2. Carotenoid data are normalized to 100 Chls ($a + b$) because Chl/polypeptide stoichiometry is not known for LHCb9. Maximum S.D. is 0.05 for Chl a/b and 0.5 for carotenoids.

	Chl *a*/Chl *b*	Carotenoids	Neoxanthin	Violaxanthin	Lutein
PpLHCb9.1	1.35	24.9	3.7	4.4	16.7
PpLHCb9.2	1.34	27.4	5.3	5.3	16.8
HvLHCb2	1.36	23.6	8.2	1.2	14.1

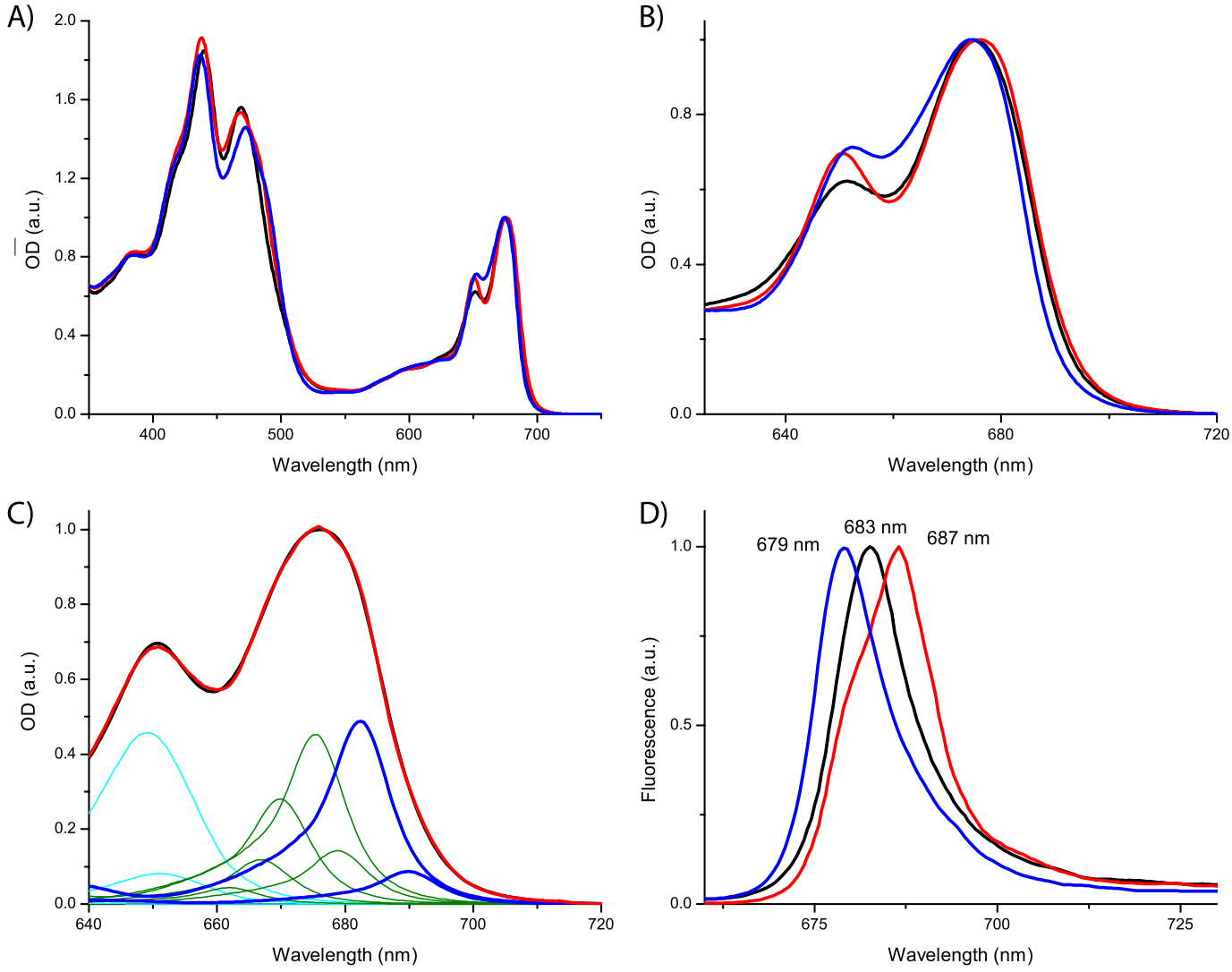

FIGURE 3. **Spectroscopic properties of LHCb9 reconstituted *in vitro*.** *A*, comparison of LHCb9.1 and LHCb9.2 absorption spectra (*black* and *red*, respectively) with barley HvLHCb2 (*blue*). *B*, red region of spectra shown in *A*. *C*, fitting of LHCb9.2 absorption spectrum (*black*) with Chl absorption forms. Chl *b* and Chl *a* forms are shown in *cyan* and *green*, respectively. The two red-most Chl *a* forms, with a maximum at 683 and 690 nm, are shown in *blue*. *D*, low temperature fluorescence spectra upon excitation at 500 nm of LHCb9.1, LHCb9.2, and barley HvLHCb2, shown in *black*, *red*, and *blue*, respectively. All spectra are normalized to the maximum value in the Q_y region. *a.u.*, arbitrary units.

mer, as found experimentally in LHCb5 and LHCb2, respectively, reconstituted *in vitro*. For all values within this interval, normalization of data in Table 1 to Chl stoichiometry suggests the presence of three carotenoid binding sites, one specific for lutein, one binding lutein or violaxanthin, and the last one specific for neoxanthin. This is similar to all LHCb1 to -5 proteins (26, 45) and is consistent with the conserved motifs from sequence analysis.

Absorption spectra showed a Chl *a* Q_y peak at 675.5 nm (Fig. 3, *A* and *B*), and an efficient energy transfer from xanthophylls and Chl *b* to Chl *a*, typical for all functional LHC proteins, was observed by the constancy of fluorescence emission spectra upon excitation at 430 nm (Chl *a*), 470 nm (Chl *b*), and 500 nm (xanthophylls) (not shown). LHCb9 absorption spectra are similar to that of HvLHCb2 (Fig. 3*A*), in agreement with their similar pigment content (44). However, the red-most part of the spectra showed differences, and both LHCb9 isoforms have a more red-shifted absorption with respect to HvLHCb2 (Fig. 3*B*). The fitting of the Q_y region of the spectrum with spectral forms of Chl *a* in a protein environment yields information on

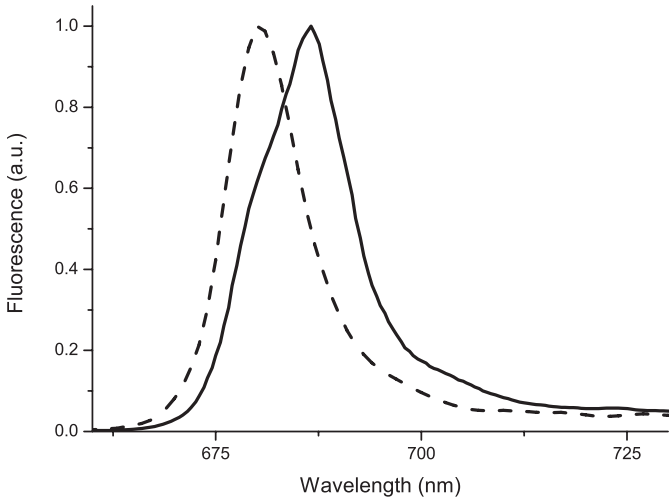

FIGURE 4. **Role of Chl 603 ligand in LHCb9 red-shifted forms.** Low temperature fluorescence spectra upon excitation at 500 nm of LHCb9.2 WT and N164H mutant are shown by a *solid* and *dashed line*, respectively. All spectra are normalized to the maximum value. *a.u.*, arbitrary units.

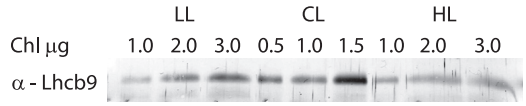

FIGURE 5. **LHCb9 accumulation in different light conditions.** Western blotting against LHCb9 in *P. patens* thylakoids purified from plants grown under different light regimes. Different dilutions of the same sample were loaded to ensure signal linearity. As indicated, to achieve similar signal intensities, different Chl amounts of low light (*LL*), control light (*CL*), and high light (*HL*) thylakoids have been loaded. *a. u.*, arbitrary units.

pigment composition and protein structure (28). In order to reconstruct LHCb9.1 and LHCb9.2 spectra, at least one red-shifted spectral form at 685–690 nm had to be introduced in order to obtain a satisfactory fitting (Fig. 3*C*). This is different from all other LHCbs, where the red-most Chl is consistently found around 680 nm using the same analysis (45). Consistent with this red-shifted absorption, the low temperature fluorescence emission spectra peaked at 683 and 687 nm, respectively, for LHCb9.1 and LHCb9.2 with respect to the 679 nm of HvLHCb2 (Fig. 3*D*). Such a property is unique among LHCb proteins, which all show very similar fluorescence emission peaks at 679–680 nm (44, 45).

Site-directed Mutagenesis on Chl 603-binding Residue of LHCb9.2—In order to verify experimentally if the red-shifted emission in LHCb9 originated from the Chl 603 as in the PSI antenna, we generated site-directed mutants substituting the asparagine ligand with a histidine, which was effective in reducing red forms in Lhca (18). The Asn to His mutation does not alter significantly the Chl binding properties, as suggested by the invariance of the Chl *a*/*b* ratio (1.29 ± 0.07 in the mutant *versus* 1.36 ± 0.05 in WT). Fluorescence emission is instead influenced and is clearly blue-shifted from 686 to 681 nm (Fig. 4). It is worth pointing out that the fluorescence emission spectrum of the Asn to His mutant is now very similar to that of other LHCb proteins, demonstrating the key role of this amino acid substitution in inducing the spectral shift.

Localization of LHCb9 in P. patens Thylakoids—In order to locate the LHCb9 polypeptides in *P. patens* thylakoids, we produced a polyclonal antibody using recombinant LHCb9.1 polypeptide as antigen. Among *P. patens* thylakoid proteins separated by SDS-PAGE, the anti-LHCb9 antibody recognized a band with apparent molecular mass of 29,300 Da (*i.e.* the mass of LHCb9 mature protein). Other bands are also highlighted in the 20–30 kDa range, where LHCs are expected to migrate (supplemental Fig. 1) and are probably due to binding to conserved LHC epitopes. To confirm this attribution, we repeated the Western blotting analysis by preincubating the antibody with LHCb9.1 and LHCb9.2 inclusion bodies. As shown in supplemental Fig. 1, the band attributed to LHCb9 is depleted by the preincubation differently from other bands with lower apparent molecular mass, implying that the upper band was indeed LHCb9. Moreover, we verified that antibodies against LHCb1 to -3, LHCb4, LHCb5, and LHCb6 (9) recognized bands with lower apparent molecular weight with respect to that identified as LHCb9 (not shown). It should be noted that the anti-LHCb9.1 did recognize both recombinant LHCb9.1 and LHCb9.2 isoforms with similar affinity, as expected from their high sequence similarity (supplemental Fig. 1).

We then proceeded to LHCb9 immunotitration in *P. patens* thylakoids in order to evaluate its approximate stoichiometry with respect to other thylakoid proteins. With this aim, we first determined the affinity of the antibody for LHCb9.1 by measuring the signal obtained from gels loaded with different amounts of recombinant LHCb9.1 reconstituted *in vitro* with pigments. On the same gel, we also loaded different amounts of thylakoid membranes (for details, see "Experimental Procedures"). Densitometric quantification showed that the same immunoblotting signal was obtained by loading 407 ± 53 Chls from thylakoids and one Chl from recombinant LHCb9.1 protein. This value can be used to estimate a stoichiometry of 0.19 ± 0.06 LHCb9 copies/PSII, by using the Chl/LHCb9 monomer and Chl/PSII values of 10 ± 2 and 788 ± 132, respectively (see "Experimental Procedures" for details). This result must be taken with some caution because it depends on several estimations; nevertheless, it suggests that LHCb9 is a significant component of *P. patens* thylakoids.

We also used the anti-LHCb9 antibody to assess if protein accumulation is modulated by light intensity during plant growth. We found that LHCb9 is more abundant in control conditions with respect to both low light and high light conditions (Fig. 5). Antenna proteins have normally similar regulatory patterns; the isoform with a preferential role in light harvesting is normally induced in low light, whereas proteins involved in photoprotection as LHCSR or PSBS are induced in strong light (8, 46, 47). Instead, here LHCb9 has a unique regulation with an increased expression in intermediate light conditions.

Localization of LHCb9 in PSII-LHCII Supercomplexes—Data presented so far showed that LHCb9.1 and/or LHCb9.2 are indeed present in *P. patens* thylakoids. Red-shifted Chl forms have not been described before in a PSII antenna protein, and this might suggest that LHCb9 is associated with PSI, despite its sequence similarity with LHCb proteins. In order to assess whether LHCb9 is associated with PSI or PSII, we fractionated thylakoid pigment-binding complexes by sucrose gradient ultracentrifugation upon solubilization with a mild detergent (Fig. 6*A*). Green bands were identified from their migration,

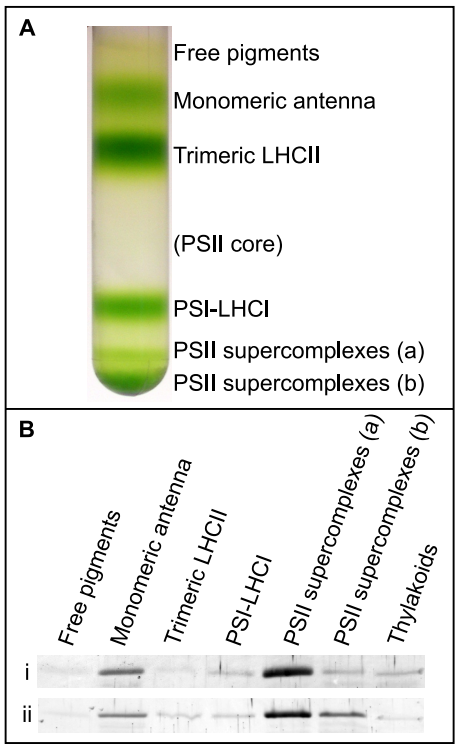

FIGURE 6. **LHCb9 distribution in *P. patens* thylakoids.** *A*, sucrose gradient ultracentrifugation pattern from solubilized thylakoids purified from plants grown in control light conditions. Pigments are distributed in six bands corresponding (from the *top*) to free pigments, monomeric and trimeric antenna proteins, and PSI-LHCI and PSII-LHCII supercomplexes of two different sizes. A seventh expected band corresponding to the PSII core is very faint. *B*, Western blotting against LHCb9 on different bands from sucrose gradient. In the first row (*i*), 1 μg of Chl was loaded in each lane, whereas in the *second row* (*ii*), the same band volume was loaded. 1 μg of Chl of thylakoids was always loaded as reference.

absorption spectra, and SDS-PAGE profile. PSI and PSII antenna complexes are well separated by this method. In fact, although LHCas are stably associated with the reaction center complex of PSI upon detergent solubilization, LHCbs are easily dissociated in two major bands corresponding to monomeric and trimeric antenna proteins, although a relevant fraction of LHCb proteins in *P. patens* migrates at the bottom of the gradient as PSII-LHCII supercomplexes (9). We tested these sucrose gradient bands for the presence of LHCb9 and found that this protein is enriched in monomeric antennas and PSII supercomplexes (Fig. 6*B*), strongly suggesting its association with PSII.

A further support for the association of LHCb9 to PSII reaction center was found by exploiting its peculiar emission at low temperature (*i.e.* red shift with respect to all other known LHCb polypeptides). This feature allows identification of this polypeptide even when it is mixed with other PSII antenna proteins. The 77 K fluorescence emission spectrum from the monomeric antenna fraction (sucrose band 2; Fig. 6*A*), enriched in LHCb9, is wider than spectra from the trimeric fraction, and a shoulder can be resolved at 685 nm in the former fraction, consistent with the LHCb9 emission (Fig. 7, *A* and *B*).

The second derivative analysis of the spectra (Fig. 7*B*) allowed highlighting of the presence of a contribution peaking at 685 nm in the monomeric fractions, which is completely missing in the trimer antenna fraction. We also noticed that the monomeric and trimeric fractions purified from *A. thaliana* thylakoids have very similar fluorescence emission spectra consistent with the absence of LHCb9 in this plant. In particular, the red-most contribution is missing, thus further strengthening the correlation between LHCb9 and the red-shifted fluorescence emission signal.

In Fig. 7*C*, the LT fluorescence of *P. patens* PSII supercomplexes is shown together with LHCb trimers and monomers, used as a reference for the absence and the presence of LHCb9, respectively. In the supercomplex spectrum, the main peak corresponds to the emission from antenna proteins, whereas a shoulder at around 695 nm is due to PSII core emission. In these samples, emissions in the 725–740 nm interval is also visible due to a small contamination from PSI-LHCI supercomplexes. The blue-most peak from the antenna, however, is clearly wider than that from LHCII trimers alone and very similar to that from monomeric antennas, consistent with a red-shifted contribution from LHCb9 in PSII supercomplexes, confirming its association with PSII-LHCII supercomplexes suggested by immunoblotting.

DISCUSSION

LHCb9 Is a New Photosystem II Antenna Polypeptide—In this work, we characterized LHCb9, a new LHC polypeptide with peculiar properties in the moss *P. patens*. Antenna polypeptides associated with PSI and PSII can be distinguished based on their amino acid sequence because of their early divergence during the evolution of plants (4, 48). We first defined this polypeptide as a photosystem II antenna because of the high similarity with LHCb antenna proteins (9). LHCb9 sequence and pigment binding prediction showed similarity to both monomeric (LHCb5) and trimeric (LHCbm) PSII antenna proteins, and thus LHCb9 could not be assigned to one or the other subgroups. Immunoblotting with an antibody directed against LHCb9, however, localized this protein in fractions containing monomeric LHCbs (LHCb4, LHCb5, and LHCb6) rather than in those containing the trimeric peripheral LHCII. Consistently, LHCb9 was found to be part of the PSII-LHCII large supercomplex (Figs. 6 and 7). Thus, although the possibility that LHCb9 transiently associates to photosystem I during state transition cannot be excluded, its identification as a genuine PSII antenna is consistent with all experimental results. Monomeric LHCbs have been localized between the PSII core complex and the peripheral antenna LHCII (49, 50). In *P. patens*, genes encoding monomeric LHCb4, LHCb5, and LHCb6 subunits are all transcribed, and the corresponding polypeptides accumulate (9). Thus, LHCb9 does not substitute completely one or more of LHCb4 to -6 in PSII-LHCII architecture. It is, however, possible that LHCb9 might take the place of LHCb4 to -6 in a fraction of PSII supercomplexes, consistent with its substoichiometric abundance with respect to the PSII core complex. Alternatively, it might bind to the PSII core in parallel with LHCb4 to -6 on the peripheral antenna layer.

Possible Physiological Role of LHCb9—LHCb9 is the only known case of a PSII antenna having an asparagine as Chl 603 ligand instead of histidine. Asparagines coordinate chlorophylls as well as histidines, but the size of the lateral chain is

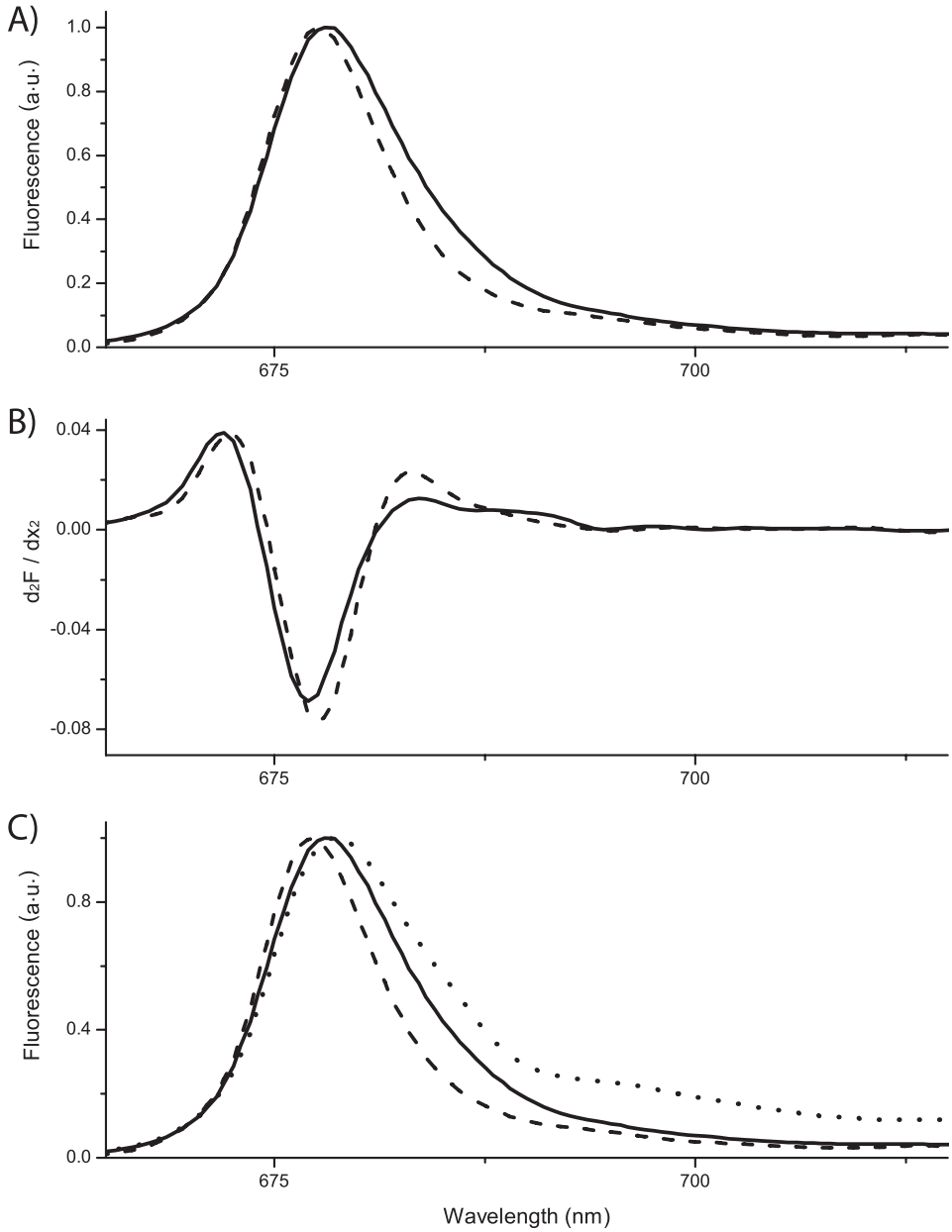

FIGURE 7. **Spectroscopic evidence for the presence of LHCb9 among *P. patens* antennas.** *A*, LT fluorescence spectra of band 2, containing monomeric LHCbs and trimeric LHCII, shown as *solid* and *dashed lines*, respectively. *B*, second derivative of spectra shown in *A*. *C*, comparison of LT spectra of bands from a sucrose gradient containing PSII-LHCII supercomplexes (*dotted line*) and monomeric (*solid line*) and trimeric (*dashed line*) antenna fractions from *P. patens*. All spectra were normalized to the peak value. Excitation was set at 500 nm. *a.u.,* arbitrary units.

smaller, bringing the ligand closer to the protein backbone. In this case, Chl 603 also becomes closer to Chl 609. In this context, the strength of the Chl-Chl interaction is higher and leads to the formation of a charge transfer state and of red-shifted Chl absorption forms (18–20). In the case of LHCb9.2, this effect can be shown by the 6-nm shift observed in fluorescence emission between the WT and Asn to His mutant (Fig. 4).

Thus, our data show that red-shifted forms are indeed present in LHCb9. It is worth underlining that although transition energies in this complex are higher than in the PSI antenna, these are nevertheless relevant because they are associated with PSII, where the reaction center energy (P680) is higher than in PSI (P700). Furthermore, trapping time is much slower in PSII than PSI, and thus any exciton delocalization is expected to have a stronger effect on photochemistry here with respect to the case of PSI. Certainly, LHCb9 significantly affects energy distribution in PSII-LHCII supercomplexes as shown by the LT fluorescence spectra; here, in fact, the LHCb9 effect can be detected despite the fact that this protein is present in far lower amounts with respect to other non-red-shifted antenna subunits (Fig. 7).

Red forms in PSI have been suggested to increase light absorption, providing an advantage in a spectrally filtered light caused by self-absorption and shading (51–53). Alternatively, red forms of PSI have been proposed to play a relevant role in PSI photoprotection by concentrating excitation energy in protein domains specialized for Chl singlet/triplet quenching (54, 55). Because an LHCb9 homologous has not yet been found in

any other plant but mosses, we might speculate that this protein plays a role related to specific environmental conditions experienced by *P. patens*. Mosses grow in a dim light environment, where red-shifted forms can provide some advantage in a shade environment when the light spectrum is altered by self-absorption (52).

As for the photoprotection role, it is worth mentioning that plants growing shaded by overhanging canopies are exposed to sudden light increase during sun flecks, a highly stressful condition leading to oxidative stress (56). It has been recently shown that the interaction between Chl 603 and Chl 609 is needed for the formation of a carotenoid radical cation whose fast recombination yields heat dissipation (57). We can thus hypothesize that red forms within the PSII antenna system of *P. patens* may also function in focusing excitons within a low energy sink, where they can be safely dissipated. As in the case of PSI, thus also for LHCb9, red-shifted Chls may play a role both in light harvesting and photoprotection, and according to analysis of protein accumulation, its effect is more helpful in intermediate light conditions. In order to verify LHCb9, this hypothesis on their physiological role, a reverse genetic analysis of the two LHCb9 isoforms is required that can be performed thanks to the unique property of *P. patens* of performing homologous recombination, as recently exploited for the determination of the function of LHCSR and PSBS proteins (58).

Acknowledgment—We thank Stefano Caffarri (Université de la Méditerranée, Marseille, France) for help with LT fluorescence spectra.

REFERENCES

1. Mozzo, M., Dall'Osto, L., Hienerwadel, R., Bassi, R., and Croce, R. (2008) *J. Biol. Chem.* **283,** 6184–6192
2. Jahns, P., Latowski, D., and Strzalka, K. (2009) *Biochim. Biophys. Acta* **1787,** 3–14
3. Horton, P., and Ruban, A. (2005) *J. Exp. Bot.* **56,** 365–373
4. Green, B. R., and Durnford, D. G. (1996) *Annu. Rev. Plant Physiol Plant Mol. Biol.* **47,** 685–714
5. Nelson, N., and Ben-Shem, A. (2005) *BioEssays* **27,** 914–922
6. Busch, A., and Hippler, M. (2011) *Biochim. Biophys. Acta* **1807,** 864–877
7. Jansson, S. (1999) *Trends Plant Sci.* **4,** 236–240
8. Klimmek, F., Sjödin, A., Noutsos, C., Leister, D., and Jansson, S. (2006) *Plant Physiol.* **140,** 793–804
9. Alboresi, A., Caffarri, S., Nogue, F., Bassi, R., and Morosinotto, T. (2008) *PLoS ONE* **3,** e2033
10. Zhang, H., Goodman, H. M., and Jansson, S. (1997) *Plant Physiol.* **115,** 1525–1531
11. Schmid, V. H., Cammarata, K. V., Bruns, B. U., and Schmidt, G. W. (1997) *Proc. Natl. Acad. Sci. U.S.A.* **94,** 7667–7672
12. Schmid, V. H., Potthast, S., Wiener, M., Bergauer, V., Paulsen, H., and Storf, S. (2002) *J. Biol. Chem.* **277,** 37307–37314
13. Castelletti, S., Morosinotto, T., Robert, B., Caffarri, S., Bassi, R., and Croce, R. (2003) *Biochemistry* **42,** 4226–4234
14. Liu, Z., Yan, H., Wang, K., Kuang, T., Zhang, J., Gui, L., An, X., and Chang, W. (2004) *Nature* **428,** 287–292
15. Kühlbrandt, W., Wang, D. N., and Fujiyoshi, Y. (1994) *Nature* **367,** 614–621
16. Ben-Shem, A., Frolow, F., and Nelson, N. (2003) *Nature* **426,** 630–635
17. Morosinotto, T., Mozzo, M., Bassi, R., and Croce, R. (2005) *J. Biol. Chem.* **280,** 20612–20619
18. Morosinotto, T., Breton, J., Bassi, R., and Croce, R. (2003) *J. Biol. Chem.* **278,** 49223–49229
19. Romero, E., Mozzo, M., van Stokkum, I. H., Dekker, J. P., van Grondelle, R., and Croce, R. (2009) *Biophys. J.* **96,** L35–L37
20. Croce, R., Chojnicka, A., Morosinotto, T., Ihalainen, J. A., van Mourik, F., Dekker, J. P., Bassi, R., and van Grondelle, R. (2007) *Biophys. J.* **93,** 2418–2428
21. Rensing, S. A., Lang, D., Zimmer, A. D., Terry, A., Salamov, A., Shapiro, H., Nishiyama, T., Perroud, P. F., Lindquist, E. A., Kamisugi, Y., Tanahashi, T., Sakakibara, K., Fujita, T., Oishi, K., Shin-I, T., Kuroki, Y., Toyoda, A., Suzuki, Y., Hashimoto, S., Yamaguchi, K., Sugano, S., Kohara, Y., Fujiyama, A., Anterola, A., Aoki, S., Ashton, N., Barbazuk, W. B., Barker, E., Bennetzen, J. L., Blankenship, R., Cho, S. H., Dutcher, S. K., Estelle, M., Fawcett, J. A., Gundlach, H., Hanada, K., Heyl, A., Hicks, K. A., Hughes, J., Lohr, M., Mayer, K., Melkozernov, A., Murata, T., Nelson, D. R., Pils, B., Prigge, M., Reiss, B., Renner, T., Rombauts, S., Rushton, P. J., Sanderfoot, A., Schween, G., Shiu, S. H., Stueber, K., Theodoulou, F. L., Tu, H., Van de Peer, Y., Verrier, P. J., Waters, E., Wood, A., Yang, L., Cove, D., Cuming, A. C., Hasebe, M., Lucas, S., Mishler, B. D., Reski, R., Grigoriev, I. V., Quatrano, R. S., and Boore, J. L. (2008) *Science* **319,** 64–69
22. Durnford, D. G., Deane, J. A., Tan, S., McFadden, G. I., Gantt, E., and Green, B. R. (1999) *J. Mol. Evol.* **48,** 59–68
23. Six, C., Worden, A. Z., Rodríguez, F., Moreau, H., and Partensky, F. (2005) *Mol. Biol. Evol.* **22,** 2217–2230
24. Guindon, S., and Gascuel, O. (2003) *Syst. Biol.* **52,** 696–704
25. Guindon, S., Lethiec, F., Duroux, P., and Gascuel, O. (2005) *Nucleic Acids Res.* **33,** W557–W559
26. Caffarri, S., Passarini, F., Bassi, R., and Croce, R. (2007) *FEBS Lett.* **581,** 4704–4710
27. Giuffra, E., Cugini, D., Croce, R., and Bassi, R. (1996) *Eur. J. Biochem.* **238,** 112–120
28. Croce, R., Canino, G., Ros, F., and Bassi, R. (2002) *Biochemistry* **41,** 7334–7343
29. Gilmore, A. M., and Yamamoto, H. Y. (1991) *Plant Physiol.* **96,** 635–643
30. Ashton, N. W., Grimsley, N., and Cove, D. J. (1979) *Planta* **144,** 427–435
31. Trouiller, B., Schaefer, D. G., Charlot, F., and Nogué, F. (2006) *Nucleic Acids Res.* **34,** 232–242
32. Ballottari, M., Govoni, C., Caffarri, S., and Morosinotto, T. (2004) *Eur. J. Biochem.* **271,** 4659–4665
33. Ballottari, M., Dall'Osto, L., Morosinotto, T., and Bassi, R. (2007) *J. Biol. Chem.* **282,** 8947–8958
34. Melis, A. (1989) *Phil. Trans. R. Soc. Lond. B* **323,** 397–409
35. Guex, N., and Peitsch, M. C. (1997) *Electrophoresis* **18,** 2714–2723
36. Bassi, R., Croce, R., Cugini, D., and Sandonà, D. (1999) *Proc. Natl. Acad. Sci. U.S.A.* **96,** 10056–10061
37. Morosinotto, T., Caffarri, S., Dall'Osto, L., and Bassi, R. (2003) *Physiol. Plant.* **119,** 347–354
38. Schmid, V. H. (2008) *Cell Mol. Life Sci.* **65,** 3619–3639
39. Hobe, S., Förster, R., Klingler, J., and Paulsen, H. (1995) *Biochemistry* **34,** 10224–10228
40. Dainese, P., Hoyer-hansen, G., and Bassi, R. (1990) *Photochem. Photobiol.* **51,** 693–703
41. Ruban, A. V., Solovieva, S., Lee, P. J., Ilioaia, C., Wentworth, M., Ganeteg, U., Klimmek, F., Chow, W. S., Anderson, J. M., Jansson, S., and Horton, P. (2006) *J. Biol. Chem.* **281,** 14981–14990
42. Elrad, D., and Grossman, A. R. (2004) *Curr. Genet.* **45,** 61–75
43. Mozzo, M., Mantelli, M., Passarini, F., Caffarri, S., Croce, R., and Bassi, R. (2010) *Biochim. Biophys. Acta* **1797,** 212–221
44. Caffarri, S., Croce, R., Cattivelli, L., and Bassi, R. (2004) *Biochemistry* **43,** 9467–9476
45. Ballottari, M., Mozzo, M., Croce, R., Morosinotto, T., and Bassi, R. (2009) *J. Biol. Chem.* **284,** 8103–8113
46. Peers, G., Truong, T. B., Ostendorf, E., Busch, A., Elrad, D., Grossman, A. R., Hippler, M., and Niyogi, K. K. (2009) *Nature* **462,** 518–521
47. Gerotto, C., Alboresi, A., Giacometti, G. M., Bassi, R., and Morosinotto, T. (2011) *Plant Cell Environ.* **34,** 922–932
48. Neilson, J. A., and Durnford, D. G. (2010) *Photosynth. Res.* **106,** 57–71
49. Boekema, E. J., van Roon, H., Calkoen, F., Bassi, R., and Dekker, J. P. (1999)

Biochemistry **38,** 2233–2239
50. Boekema, E. J., Van Roon, H., Van Breemen, J. F., and Dekker, J. P. (1999) *Eur. J. Biochem.* **266,** 444–452
51. Trissl, H. W. (1993) *Photosynth. Res.* **35,** 247–263
52. Rivadossi, A., Zucchelli, G., Garlaschi, F. M., and Jennings, R. C. (1999) *Photosynth. Res.* **60,** 209–215
53. Matsubara, S., Morosinotto, T., Osmond, C. B., and Bassi, R. (2007) *Plant Physiol.* **144,** 926–941
54. Carbonera, D., Agostini, G., Morosinotto, T., and Bassi, R. (2005) *Biochemistry* **44,** 8337–8346
55. Alboresi, A., Ballottari, M., Hienerwadel, R., Giacometti, G. M., and Morosinotto, T. (2009) *BMC Plant Biol.* **9,** 71
56. Watling, J. R., Robinson, S. A., Woodrow, I. E., and Osmond, C. B. (1997) *Aust. J. Plant Physiol.* **24,** 17–25
57. Ahn, T. K., Avenson, T. J., Ballottari, M., Cheng, Y. C., Niyogi, K. K., Bassi, R., and Fleming, G. R. (2008) *Science* **320,** 794–797
58. Alboresi, A., Gerotto, C., Giacometti, G. M., Bassi, R., and Morosinotto, T. (2010) *Proc. Natl. Acad. Sci. U.S.A.* **107,** 11128–11133